3-29-2010

A grazing incidence x-ray streak camera for ultrafast, single-shot measurements

J. Feng

K. Engelhorn

B. I. Cho

H. J. Lee

M. Greaves

See next page for additional authors

Recommended Citation

Feng, J., Engelhorn, K., Cho, B. I., Lee, H. J., Greaves, M., Weber, C. P., … Heimann, P. A. (2010). A grazing incidence x-ray streak camera for ultrafast, single-shot measurements. Applied Physics Letters, 96(13), 134102. https://doi.org/10.1063/1.3371810

Authors
J. Feng, K. Engelhorn, B. I. Cho, H. J. Lee, M. Greaves, Christopher P. Weber, R. W. Falcone, H. A. Padmore, and P. A. Heimann

A grazing incidence x-ray streak camera for ultrafast, single-shot measurements

J. Feng,[a] K. Engelhorn, B. I. Cho, H. J. Lee,[b] M. Greaves, C. P. Weber,[c] R. W. Falcone, H. A. Padmore, and P. A. Heimann
Lawrence Berkeley National Laboratory, Berkeley, California 94720, USA

(Received 18 February 2010; accepted 3 March 2010; published online 29 March 2010)

An ultrafast x-ray streak camera has been realized using a grazing incidence reflection photocathode. X-rays are incident on a gold photocathode at a grazing angle of 20° and photoemitted electrons are focused by a large aperture magnetic solenoid lens. The streak camera has high quantum efficiency, 600 fs temporal resolution, and 6 mm imaging length in the spectral direction. Its single shot capability eliminates temporal smearing due to sweep jitter, and allows recording of the ultrafast dynamics of samples that undergo nonreversible changes. © *2010 American Institute of Physics*. [doi:10.1063/1.3371810]

An x-ray streak camera has the unique feature that it allows the simultaneous recording of ultrafast temporal information on a subpicosecond time scale as well as spectral information using a two-dimensional charge-coupled device (CCD) detector.[1,2] X-ray streak cameras have been used to study ultrafast dynamics in solids and in warm dense matter (WDM) at third generation synchrotron facilities.[2–4] Over the past decade, different ideas have been proposed and carried out to improve the temporal resolution of x-ray streak cameras.[5–10] Improvement of the quantum efficiency of streak cameras, however, has made little progress. The quantum efficiency of a streak camera is a key parameter for experiments, such as ultrafast dynamics of WDM where the sample is ablated with each shot.[11,12] To date, most x-ray streak cameras use the transmission geometry for a photocathode to generate photoelectrons. In the transmission geometry, light is incident on the photocathode from the front side and the photoelectrons emit from the back side of the photocathode. A very thin photocathode has to be used in this operational mode. The incident light must penetrate the cathode substrate and the generated photoelectrons are scattered in the whole depth of the cathode material. Due to the mismatch of x-ray penetration depth and the secondary electron mean free path in the photocathode, the quantum efficiency is low, and this results in the need to operate in accumulation mode over many shots. However, Lowney *et al.*[13] showed that the total photoelectron yield and quantum efficiency of a photocathode increases as the x-ray penetration depth approaches the secondary electron mean free path. A streak camera can have therefore very high quantum efficiency when the photocathode is in grazing incidence reflection geometry in order to facilitate this matching condition. In this letter, we describe a grazing incidence x-ray streak camera with very high quantum efficiency, wide spectral range, and ultrafast temporal resolution.

A schematic diagram of the grazing incidence streak camera used in this work is shown in Fig. 1. There are two entrances which are aligned 20° with respect to the photocathode surface on the opposite side of the streak camera. One is used for x-ray illumination and the other for time calibration provided by UV pulses derived from an ultrafast laser. Due to the reflection geometry, thick materials can be coated on a bulk substrate for use as the photocathode. We tested cesium iodide (CsI) and gold (Au) photocathodes of various coating thicknesses. We found that CsI photocathodes suffer from radiation damage after ~30 minutes exposure with a flux of 2×10^{12} photons/sec/mm^2 at 300 eV at the Advanced Light Source (ALS) undulator beamline 6.0.2.[14] Our transmission geometry Au photocathode also damaged rapidly (~30 min) when it was exposed to the undulator x-ray beam. This damage may be caused by the thermal cycling of the thin Au coating on a thin substrate by the pulsed x-ray beam. We therefore used Au with ~600 nm thickness coated on a thick, fused silica substrate of 1 inch in diameter. The Au photocathode withstood the very high brightness of the beamline 6.0.2 and worked robustly for weeks of x-ray exposure. A mesh anode is placed downstream facing the Au coated surface. The mesh anode generates a uniform high gradient field of ~10 MV/m between the photocathode and anode. Slits of various sizes are placed after the mesh anode, and are used to define the electron source size. The deflection plates are put within a few mm of the photocathode in order to have a small electron bunch beam size entering the deflection plates, thereby reducing deflection aberrations. A compact magnetic solenoid lens is located after the deflection plates, and was designed with a large opening aperture using the COSY particle tracking code[15] in order to reduce field aberrations.

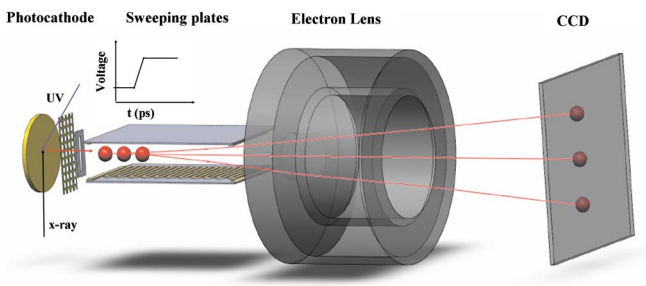

FIG. 1. (Color online) Schematic of the grazing incidence streak camera.

[a]Electronic mail: fjun@lbl.gov.
[b]Present address: SLAC National Accelerator Laboratory, Menlo Park, CA 94025.
[c]Present address: Department of Physics, Santa Clara University, Santa Clara, CA 95053.

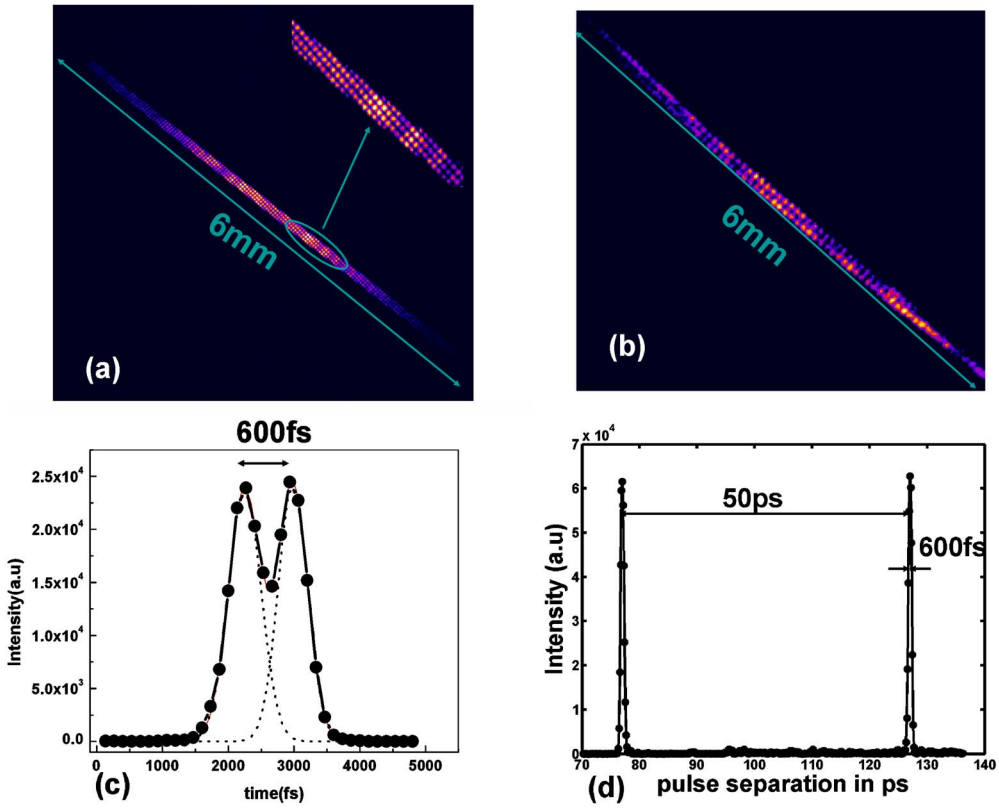

FIG. 2. (Color online) The measured performance of the grazing incidence streak camera. (a) Static image of 100 um (in the time dispersion direction) by 6 mm (in the spectral direction) slit illuminated with 266 nm UV light. The anode mesh is 750 lines/inch. The inset image is zoomed in a small area. (b) Streak image for two UV pulses separated by 600 fs. (c) Projected streak image for two UV pulses separated by 600 fs. Dotted lines are fitted by a Gaussian distribution. (d) Projected streak image for two UV pulses separated by 50 ps.

The experimental setup for testing the streak camera is similar to that in Ref. 1. The 790 nm, 1 mJ and 30 fs laser beam from a Ti:sapphire laser is split into two beams. One beam is frequency tripled into 4.7 eV UV light by using a beta barium borate nonlinear crystal system. Then the generated UV light is sent to a computer controlled delay stage. The UV pulse is equally divided into two pulses, which are sent through a Mach–Zehnder interferometer for time calibration. The two UV pulses enter the streak camera chamber collinearly at 20° with respect to the photocathode surface to generate photoelectrons. The other 790 nm beam from the beam splitter is incident on a GaAs photoconductive switch. Two high voltage pulses with approximately 400 V are output from the photoconductive switch and are used to drive a pair of meander line deflection plates in the streak camera. The synchronization of the high voltage pulses and the photoelectrons is accurately controlled by the delay stage to give the best sweep speed.

The temporal resolution Δt of the grazing incidence reflection streak camera is given approximately as a quadratic sum of different components as follows:

$$\Delta t = \sqrt{\Delta t_d^2 + \Delta t_{\text{sweep-slit}}^2 + \Delta t_{\text{jitter}}^2 + \Delta t_{sc}^2 + \Delta t_\theta^2}, \quad (1)$$

where Δt_d is due to time dispersion from the energy spread of the photoemitted electrons, $\Delta t_{\text{sweep-slit}}$ is related to finite static image size and deflection sweeping speed, Δt_{jitter} is pulse-to-pulse jitter due to the laser energy fluctuations on the photoconductive switch and becomes zero for single-shot measurements, Δt_{sc} is due to space charge effects among the electrons, and Δt_θ is due to the optical path difference of light at grazing incidence angle θ. The most important term, Δt_d is 186 fs with 10 kV/mm accelerating gradient field and UV illumination, for which the secondary electron energy distribution has a 0.5 eV energy width; for x-rays, Δt_d is 526 fs, where secondary electrons have a 4 eV energy width. The last term in Eq. (1), Δt_θ, is added for the reflection geometry streak camera. Δt_θ can be written as

$$\Delta t_\theta = \frac{d \cos(\theta)}{c}, \quad (2)$$

where d is the slit size in the temporal direction, c is the speed of light. For example, Δt_θ is 78 fs for a 25 μm slit size at 20°.

Figures 2 and 3 report demonstrations of our streak camera performance. Figure 2 shows the measured performance of the grazing incidence streak camera using 4.7 eV UV light which was used because of the unavailability of a suitable ultrafast x-ray source. Figure 2(a) shows the spatial resolution of the streak camera in static mode by imaging the anode mesh without voltage ramps on the deflection plates. A 2.21 A current is used for the magnetic solenoid lens to get good focus, which agrees with the COSY calculation. The inset image is zoomed in a small area as shown in the figure. The anode is a 750 line/inch Cu mesh that generates a uni-

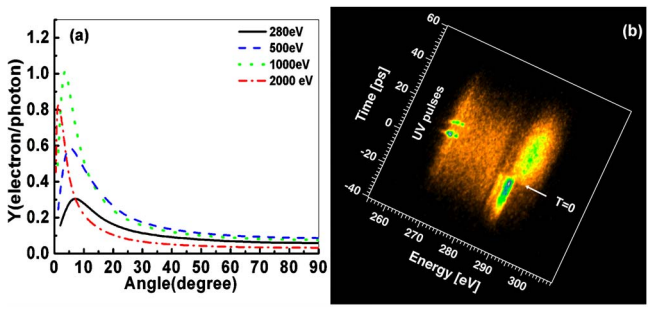

FIG. 3. (Color online) (a) Calculated total electron yield vs incidence angle from Au photocathode excited by 280, 500, 1000, and 2000 eV photons. (b) A single-shot streaked x-ray image of laser heated diamond. Two UV pulses used for time calibration are also visible. Time zero, when the dynamics are triggered by the pump laser, is clearly observed.

form high gradient accelerating field. The mesh has an effective opening size of 25 μm separated by 8 μm wide wires. The slit size is 6 mm along the direction of spectral dispersion. To illuminate the 6 mm slit in the spectrum direction, the UV beam is not focused. In the figure, the image brightness changes with the UV intensity distribution. The 8 μm wide wires are clearly resolved along the whole 6 mm length in the spectrum direction.

The performance of the streak camera in the dynamic mode is shown in Fig. 2(b) for a slit of 25 μm in the time dispersion direction. The two UV pulses are separated by 600 fs and are clearly resolved. The temporal resolution remains good along the entire spectra length, and the spatial resolution is nearly as good as in static mode. The focus current for the solenoid lens stays unchanged for both static and dynamic mode, which shows that the deflection aberration is small. Figure 2(c) shows the image profiles of Fig. 2(b) projected onto the time axis. The dotted lines are fits to a Gaussian distribution with width 480 fs. The pulse distribution is approximately Gaussian in shape. The high temporal and spatial resolutions of the streak camera can be maintained in a time window of 50 ps (which is the travel limitation of our interferometer) as shown in the Fig. 2(d). This feature is important when using synchrotron light, as the synchrotron pulse duration is several tens of picoseconds.

The quantum efficiency of a photocathode can be described using the total electron yield, i.e., the average number of electrons produced per incident photon. The total electron yield Y for a photocathode of thickness T, at a grazing angle α with respect to the surface is[13]

$$Y = E_{ph}\varepsilon^{-1}\mu \csc \alpha'[1 - R(\alpha)]P_s(0)\int_0^T \exp[-z(\mu \csc \alpha' + L_s^{-1})]dz, \quad (3)$$

where E_{ph} is x-ray energy, ε is energy required to promote a single electron from the valence band with sufficient energy to escape the photocathode, μ is the energy dependent linear absorption coefficient, α' is the angle the refracted x ray makes with respect to the photocathode surface, $R(\alpha)$ is the Fresnel reflectivity, $P_s(0)$ is the electron escape probability at the surface, and L_s is the mean-free-path of the secondary electrons. For Au photocathode, previous work has shown that a good fit to experimental data can be given with $\varepsilon = 8$ eV, $P_s(0) = 0.03$, and $L_s = 20$ Å.[16] The x-ray attenuation length $(\mu \csc \alpha')^{-1}$ and the x-ray reflectivity $R(\alpha)$ can be calculated from Ref. 17. Figure 3(a) shows the electron yield Y of Au photocathode as a function of incident angles for 280, 500, 1000, and 2000 eV incident photons calculated using Eq. (3). The yield increases with decreasing grazing angle, until the cathode becomes reflective at small angles. For example, the quantum efficiency of a Au photocathode for 3° grazing incidence angle at 1000 eV photon energy increases by a factor of 15 compared to that of normal incidence. Below 10°, the yield decreases due to increased reflectivity from the cathode. We chose 20° as the grazing incidence angle for our reflection streak camera as a compromise between high quantum efficiency, temporal resolution, and spectra resolution.

Figure 3(b) shows a single-shot streaked spectrum of a diamond sample using a single synchrotron pulse from ALS beamline 6.0.2. An additional intense, ultrashort laser pulse is focused onto the sample and synchronized with a broadband x-ray pulse that is transmitted through the sample. The laser melts the sample with extreme temperature and pressure and a WDM state is formed. The x-ray probe pulse passes through the sample, and then is dispersed, and the spectrum is measured as a function of energy and time by the streak camera. Two UV pulses separated by 1 mm are used to calibrate the time and to monitor the performance of the streak camera during the experiment. The time zero t=0 shown in the Fig. 3(b) is defined to be the time when the laser hits the sample and WDM dynamics starts. It is clearly visible that there is a large and abrupt change at and after time zero in the single shot streaked spectrum. The grazing incidence streak camera has been used robustly for WDM dynamics experiments on amorphous carbon, diamond, SiO_2, and Cu samples at beamline 6.0.2.

In summary, an ultrafast x-ray streak camera using a 20° grazing incidence angle has been developed. The photocathode of the streak camera has a reflection geometry and uses extraction-mesh acceleration as well as a large aperture magnetic solenoid lens. The streak camera has demonstrated very high quantum efficiency, spectral and temporal resolutions simultaneously, enabling a single shot measurement of ultrafast dynamics using a single synchrotron x-ray pulse.

This work was supported by the Director, Office of Science, Office of Basic Energy Sciences, of the U.S. Department of Energy under Contract No. DE-AC02-05CH11231. The authors would like to thank D. Lowney, Z. Hao, and A. MacPhee for an early stage of the grazing incidence streak camera design, W. Wan for COSY calculation, and E. M. Gullikson and F. Salmassi for coating the photocathode.

[1] J. Feng, H. J. Shin, J. R. Nasiatka, W. Wan, A. T. Young, G. Huang, A. Comin, J. Byrd, and H. A. Padmore, Appl. Phys. Lett. **91**, 134102 (2007).
[2] A. F. Bartelt, A. Comin, J. Feng, J. R. Nasiatka, T. Eimüller, B. Ludescher, G. Schütz, H. A. Padmore, A. T. Young, and A. Scholl, Appl. Phys. Lett. **90**, 162503 (2007).
[3] A. M. Lindenberg, I. Kang, S. L. Johnson, T. Missalla, P. A. Heimann, Z. Chang, J. Larsson, P. H. Bucksbaum, H. C. Kapteyn, H. A. Padmore, R. W. Lee, J. S. Wark, and R. W. Falcone, Phys. Rev. Lett. **84**, 111 (2000).
[4] S. L. Johnson, P. A. Heimann, A. M. Lindenberg, H. O. Jeschke, M. E. Garcia, Z. Chang, R. W. Lee, J. J. Rehr, and R. W. Falcone, Phys. Rev. Lett. **91**, 157403 (2003).
[5] M. M. Shakya and Z. Chang, Appl. Phys. Lett. **87**, 041103 (2005).
[6] J. Feng, W. Wan, J. Qiang, A. Bartelt, A. Comin, A. Scholl, J. Byrd, R. Falcone, G. Huang, A. MacPhee, J. Nasiatka, K. Opachich, D. Weinstein, T. Young, and H. A. Padmore, Proc. SPIE **5920**, 592009 (2005).
[7] J. Qiang, J. M. Byrd, J. Feng, and G. Huang, Nucl. Instrum. Methods **A598**, 465 (2009).
[8] J. D. Hares and A. K. L. Dymoke-Bradshaw, Rev. Sci. Instrum. **79**, 10F502 (2008).
[9] P. Musumeci, J. T. Moody, C. M. Scoby, M. S. Gutlerrez, and T. Tran, Rev. Sci. Instrum. **80**, 013302 (2009).
[10] P. A. Jaanimagi, Proc. SPIE **5194**, 171 (2004).
[11] Y. Ping, D. Hanson, I. Koslow, T. Ogitsu, D. Prendergast, E. Schwegler, G. Collins, and A. Ng, Phys. Rev. Lett. **96**, 255003 (2006).
[12] R. Ernstorfer, M. Harb, C. T. Hebeisen, G. Sciaini, T. Dartigalongue, and R. J. D. Miller, Science **323**, 1033 (2009).
[13] D. P. Lowney, P. A. Heimann, E. M. Gullikson, A. G. Macphee, and R. W. Falcone, Rev. Sci. Instrum. **75**, 3131 (2004).
[14] P. A. Heimann, T. E. Glover, D. Plate, H. J. Lee, V. C. Brown, H. A. Padmore, and R. W. Schoenlein, AIP Conf. Proc. **879**, 1195 (2007).
[15] M. Berz, Nucl. Instrum. Methods **A298**, 473 (1990).
[16] G. W. Fraser, M. T. Pain, J. E. Lees, C. R. Binns, J. F. Pearson, and P. R. Houghton, Nucl. Instrum. Methods **A321**, 385 (1992).
[17] B. L. Henke, E. M. Gullikson, and J. C. Davis, At. Data Nucl. Data Tables **54**, 181 (1993).